2-45-20

THREE-DIMENSIONAL FREE SURFACE MODEL FOR THERMAL DISCHARGE

S.Lee, S. Sengupta, C. Tsai, H.Miller
Dept. of Mechanical Engineering
University of Miami
Coral Gables, Florida U.S.A.

(A) INTRODUCTION

As the result of economic and population growth, the demand for electrical power has been doubling every decade since World War II in the U.S. The rapid increase both in electricity production and in the unit size of thermal power plants has resulted in use of large quantities of water for cooling purposes. The most common system for heated effluents dsposal is the open cycle system where the condenser cooling water is discharged back into the natural waterway. Analysis of thermal discharge with a view to decreasing environmental effects and increasing the cooling efficiency has become an important part of power plant siting evaluations.

In the past years, numerical models have been developed by many researchers for predicting the velocity and temperature distribution in thermal plumes, such as Wada (1969), Koh and Fan (1971), Stolzenbach and Harleman (1972),Waldrop and Farmer (1974), Paul and Lick (1973) etc. A review of existing models is presented by Dunn and Policastro (1975). Most of the existing models cannot adequately account for time-dependent, three-dimensional flow fields, realistic bottom topography effects, and surface wave phenomenon. Since a buoyant plume is three-dimensional in character and is significantly effected by bottom topography, ambient currents and local meteorology, the need for "complete models" is acute.

A time-dependent, three-dimensional, free-surface, numerical model with both horizontal and vertical stretching has been developed for the thermal discharge study, and is presented in this paper. The effects of variable bottom topography, free surface elevations, surface heat transfer, currents, and meteorological conditions are considered in this model. The model can simulate the physical conditions needed to provide sufficient three-dimensional information for the studies of water quality to meet the appropriate standards. The model is not only a flexible and economical tool for the heated water disposal system design or improvement consideration, but also for monitoring thermal effects

in the receiving domain.

Numerical integration of the governing equations (conservation of mass, conservation of momentum, and energy) is performed simultaneously by using finite difference approximations for the differential equation. Both surface and submerged types of discharge systems in a bay and coastal site have been modelled. The results from the computer model were compared satisfactorily both with airborne thermal scanner remote sensing data and in-situe ground truth measurements at Florida Power & Light Company's Cutler Ridge Plant and Hutchinson Island Nuclear Power Plant. Only the results for Hutchinson Island site will be presented here. The application of this model to a specific site, involves specification of initial conditions, boundary conditions, and information geometry of the discharge.

(B) FORMULATION AND BASIC EQUATIONS

Numerical modeling of heated water discharges involves the application of fundamental hydrodynamic and thermodynamic equations. Several assumptions have been made for this study, namely,

(1) The fluid flow is incompressible,
(2) The fluid flow is turbulent and that the molecular transport can be neglected in comparison with turbulent transport, approximated by eddy transport coefficients,
(3) Pressures are hydrostatic throughout the whole domain,
(4) The solid wall and bottom are adiabatic, and
(5) The density throughout the flow field is a function of temperature only.

A vertical coordinate transformation technique similar to Phillips (1957) is used to incorporate both free surface and variable bottom topography and the same number of grid points in vertical direction can be used in the model. The new sigma vertical coordinate system is obtained by letting

$$\sigma = \frac{Z\ (x,y,z,t)}{H\ (x,y,t)} = \frac{z + \eta\ (x,y,t)}{h\ (x,y) + \eta\ (x,y,t)}$$

where $Z = Z\ (x,y,z,t)$ is the position of the fluid element relative to the free surface, $H = H\ (x,y,t)$ is the depth contour relative to the free surface, z represents the vertical position relative to the mean water level, η is the free surface elevation measured positively upward from mean water level, h represents the depth relative to the mean water

level. The value of σ ranges from zero at free surface to unity at the bottom of the basin. This mathematical technique has been used for a variety of numerical models of geophysical fluid flow, e.g., Smagorinsky (1965), Arakawa (1972), for the atmosphere study and Freeman (1972), Sengupta and Lick (1974) for the study of lakes. Fig. 1 and Fig. 2 show the two coordinate systems before and after vertical coordinate transformation respectively.

It is desireable to obtain a more detailed description of the flow near the discharging area and meanwhile a large horizontal domain can be covered. If a constant grid size were used, then a large number of grid points and excessive computation time are needed for the model. In order to solve this problem, a horizontal stretching is used in both lateral and transverse directions to create a small grid size near the discharge area and larger grid size away from the discharge points. An arc-tangent equation was used by Waldrop and Farmer (1974) as the horizontal stretching. A hyperbolic sine stretching has been used in this study for both lateral and transverse directions, as shown below:

$$x = a + C_1 \sinh \left[C_2 (X - d) \right]$$

$$y = b + C_3 \sinh \left[C_4 (Y - e) \right]$$

where x, y are the real coordinate; X,Y are the stretched coordinate; a and b are the distance at which the minimum step size is desired; C_1, C_2, C_3, C_4, d,e, are the constants to be determined by the imposed conditions. By using this horizontal stretching, even increments of ΔX and ΔY can be used in the model for the variable physical grid sizes.

Applying the differential transformation relationships, the horizontal and vertical stretched governing equations in the $XY\sigma$ coordinate are:

Continuity Equation

$$\frac{\partial H}{\partial t} + X' \frac{\partial (Hu)}{\partial X} + Y' \frac{\partial (Hv)}{\partial Y} + H \frac{\partial \Omega}{\partial \sigma} = 0 \quad \ldots\ldots\ldots\ldots (1)$$

Momentum Equation

u - momentum:

$$\frac{\partial (Hu)}{\partial t} + X' \frac{\partial (Huu)}{\partial X} + Y' \frac{\partial (Huv)}{\partial Y} + H \frac{\partial (u\Omega)}{\partial \sigma} =$$

$$H\left[-\frac{X'}{\rho}\left(\frac{\partial P}{\partial X}\right)+gX'\left(\sigma\frac{\partial H}{\partial X}-\frac{\partial \pi}{\partial X}\right)+f v\right]$$

$$+K_H\left[(X')^2\frac{\partial H}{\partial X}\frac{\partial u}{\partial X}+H(X')^2\frac{\partial^2 u}{\partial X^2}+HX''\frac{\partial u}{\partial X}\right]$$

$$+K_H\left[(Y')^2\frac{\partial H}{\partial Y}\frac{\partial u}{\partial Y}+H(Y')^2\frac{\partial^2 u}{\partial Y^2}+HY''\frac{\partial u}{\partial Y}\right]$$

$$+\frac{1}{\rho}\left[\frac{\partial}{H\partial\sigma}\left(\rho K_v\frac{\partial u}{\partial\sigma}\right)\right] \quad \ldots\ldots\ldots\ldots\ldots\ldots\ldots\ldots\ldots\ldots(2)$$

v - momentum:

$$\frac{\partial(Hv)}{\partial t}+X'\frac{\partial(Huv)}{\partial X}+Y'\frac{\partial(Hvv)}{\partial Y}+H\frac{\partial(v\Omega)}{\partial\sigma}=$$

$$H\left[-\frac{Y'}{\rho}\left(\frac{\partial P}{\partial Y}\right)+gY'\left(\sigma\frac{\partial H}{\partial Y}-\frac{\partial \pi}{\partial Y}\right)-f u\right]$$

$$+K_H\left[(X')^2\frac{\partial H}{\partial X}\frac{\partial v}{\partial X}+H(X')^2\frac{\partial^2 v}{\partial X^2}+HX''\frac{\partial v}{\partial X}\right]$$

$$+K_H\left[(Y')^2\frac{\partial H}{\partial Y}\frac{\partial v}{\partial Y}+H(Y')^2\frac{\partial^2 v}{\partial Y^2}+HY''\frac{\partial v}{\partial Y}\right]$$

$$+\frac{1}{\rho}\left[\frac{\partial}{H\partial\sigma}\left(\rho K_v\frac{\partial v}{\partial\sigma}\right)\right] \quad \ldots\ldots\ldots\ldots\ldots\ldots\ldots\ldots\ldots\ldots(3)$$

Energy Equation

$$\frac{\partial(HT)}{\partial t}+X'\frac{\partial(HuT)}{\partial X}+Y'\frac{\partial(HuT)}{\partial Y}+H\frac{\partial(\Omega T)}{\partial\sigma}$$

$$=B_H\left[(X')^2\frac{\partial H}{\partial X}\frac{\partial T}{\partial X}+H(X')^2\frac{\partial^2 T}{\partial X^2}+HX''\frac{\partial T}{\partial X}\right]$$

$$+B_H\left[(Y')^2\frac{\partial H}{\partial Y}\frac{\partial T}{\partial Y}+H(Y')^2\frac{\partial^2 T}{\partial Y^2}+HY''\frac{\partial T}{\partial Y}\right]$$

$$+\frac{1}{\rho H}\left[\frac{\partial}{\partial\sigma}\left(\rho B_v\frac{\partial T}{\partial\sigma}\right)\right] \quad \ldots\ldots\ldots\ldots\ldots\ldots\ldots\ldots\ldots\ldots(4)$$

Equation of State

$$\rho = F(T) = 1.000428 - 0.000019T - 0.000036T^2 \quad \ldots\ldots\ldots (5)$$

The relationship between real vertical velocity and vertical velocity in σ coordinate is derived as follows:

$$w = H\Omega + (\sigma - 1)\frac{d\eta}{dt} + \sigma\left(uX'\frac{\partial h}{\partial X} + vY'\frac{\partial h}{\partial Y}\right) \quad \ldots\ldots\ldots (6)$$

By integrating the continuity equation with respect to σ from surface to bottom we can get

$$\frac{\partial H}{\partial t} = -\int_o^1 \left[X'\frac{\partial (Hu)}{\partial X} + Y'\frac{\partial (Hv)}{\partial Y}\right] d\sigma - \left(w_b - u_b X'\frac{\partial h}{\partial X} - v_b Y'\frac{\partial h}{\partial Y}\right) \quad \ldots\ldots\ldots (7)$$

Substitute the above equation into continuity equation and integrate from surface to $\sigma = \sigma$, and the result can be obtained as

$$\Omega = \frac{1}{H}\int_o^\sigma \left[X'\frac{\partial (Hu)}{\partial X} + Y'\frac{\partial (Hv)}{\partial Y}\right] d\sigma + \frac{\sigma}{H}\int_o^1 \left[X'\frac{\partial (Hu)}{\partial X} + Y'\frac{\partial (Hv)}{\partial Y}\right] d\sigma + \frac{\sigma}{H}\left(w_b - u_b X'\frac{\partial h}{\partial X} - v_b Y'\frac{\partial h}{\partial Y}\right) \quad \ldots\ldots\ldots (8)$$

where subscript b denotes at the bottom of basin and

$$X' = \frac{dX}{dx} \; ; \; Y' = \frac{dY}{dy}$$

$$X'' = \frac{d^2X}{dx^2} \; ; \; Y'' = \frac{d^2Y}{dy^2}$$

The hydrostatic relationship is used as the diagnostic equation for pressure

$$P(\sigma) = P(0) + gH\int_o^\sigma \rho(\sigma)\, d\sigma \quad \ldots\ldots\ldots (9)$$

where P (0) is the pressure at the free surface.

(C) INITIAL AND BOUNDARY CONDITIONS

In order to solve the set of governing equations, the initial and boundary conditions should be specified throughout the whole domain. This information may be obtained from remote sensing data, in-situ measurement and other sources. Boundary conditions are specified at the air-water interface, the bottom of basin, the lateral solid walls, discharge points, and open boundaries. At the air-water interface the wind stress and the heat transfer coefficient are specified. The condition of no slip at lateral solid wall and bottom of basin is used for the momentum equations.

At solid lateral walls and at the bottom of basin, adiabatic conditions are assumed. At points of thermal discharge, both velocity and temperature are specified. The domain is bound on three sides by open boundaries where conditions are most difficult to specify. At these boundaries, the outflow velocity gradient normal to boundary is considered zero and the inflow velocities are the known values. For the temperature, the second derivative is equated to zero for outflow, implying no diffusive heat transfer and convective heat transfer is dominated. For the inflow, the temperature is the same as ambient water temperature.

(D) METHOD OF SOLUTION

The set of governing equations are unsteady, non-linear and second order partial differential equations. With the widespread use of the high-speed digital computers, finite difference approximation methods for the partial differentiation are used for solving the numerical solution.

In the three-dimensional free surface model, central differencing is used for the space derivatives in the interior of the basin. Single-sided differencing is used for the space derivatives at the boundary. Forward differencing in time for the first time step and then the central differencing in time is used for predicting the new values of all the dependent variables. In order to insure the numerical stability, the convective terms, pressure term and Coriolis force term are calculated by using the values at present time, the viscous terms are calculated by using the values at previous time step $(t-\Delta t)$. All the dependent variables are computed at integral grid points of the basin.

A two-dimensional matrix (MAR) was created in the computation process for locating the position in the basin to insure the appropriate numerical scheme and boundary conditions are used

in the computation. Different values of MAR were assigned to the different locations in the basin, such as MAR = 11 reprents the points in the interior, and MAR = 0 represents points outside the domain.

The finite difference form of governing equations is solved simultaneously for each time step. Before the computation process, the initial conditions for all the dependent variables should be specified throughout the domain. The surface heights are computed from the vertically integrated continuity equation. The horizontal velocities are computed directly from the momentum equation. The vertical velocities are obtained from new horizontal velocities and surface heights into equation (6). The temperatures are calculated from the energy equation. The pressures are obtained from the hydrostatic relationship. This procedure is performed at each time step until the desired length of time has been achieved.

(E) APPLICATION

The three-dimensional free surface model has been applied to FPL's Hutchinson Island Nuclear Power Plant which is located about midway between the cities of Fort Pierce and Stuart on the eastern ocean coast of Florida. The objective of this study is to use this model to predict the velocity and temperature distribution caused by a submerged thermal discharge into the ocean under various environmental conditions. The 12 feet diameter submerged discharge pipeline is buried in the ocean bed and terminates at a point about 1200 feet offshore at a depth of 18 feet from mean water level. At its termination, a two port Y-type discharge is added with each arm being 7.5 feet in diameter. A short sloping concrete pan is located at the outlet to prevent scouring of the ocean floor. The submerged jet discharge exits horizontally with a relatively high velocity and rises to the surface owing to buoyancy effects and then spreads out by the action of turbulent mixing and ambient currents.

A numerical grid system of 20 x 20 in the horizontal plane and five grids in the vertical plane were chosen. The domain covered is 2000 meters parallel to the shore line and 2380 meters perpendicular to the shore (along the discharge pipe axis). Fig. 4 shows a vertical section along the discharge pipe axis, the vertical and horizontal stretching and its influence on the numerical grid system is apparent.

On June 2, 1976, the heated water had an exit velocity of 280 cm/sec (9.1 ft/sec) at each end of the Y-type discharging

pipe. The ambient water temperature was about 25.5°C, discharge water temperature was 35°C, and air temperature was 29°C. The wind speed was 10 mph from the southeast. The ocean current was about 25 cm/sec predominantly northerly. The discharge conditions and the environmental conditions were incorporated into the model. It was found that the plume rapidly rises to the surface and spreads to the north owing to the current.

Fig. 5 shows the surface velocities predicted for environmental conditions of June 2, 1976. The imposed northerly current prevails away from the discharge and near the discharge points there is a source-like flow pattern because the plume rapidly rises to the surface and spreads. Fig. 6 shows the horizontal velocity on the plane 6.5 meters below the mean water level. The Y-type discharge pipe discharged horizontally with a relatively high velocity as can be seen at the discharge points, and then turned with the current. Fig. 7 shows the velocity distributions of the vertical section along the discharge pipe axis. The vortex just west of the discharge caused by the entrainment is clearly evident. Fig. 8 shows the velocity distributions of the vertical section I = 10 that is parallel to the shore line. The plume rises to the surface owing to the buoyancy and then is carried along with the current.

Fig. 9 shows the isotherms of a vertical section I = 9 that is perpendicular to the axis of the discharge pipe. The plume rises to the surface and then spreads out and is carried along with the current as is evident. Fig. 10 shows the surface isotherms from I.R. data in the morning at Hutchinson Island Power Plant on June 2, 1976. The submerged plume reises to the surface and spreads with the northerly current. The morning I.R. data base was used as the initial conditions for the model and the afternoon results were predicted by the model. The plume shifted eastwards during this period and the area of 26.5°C isotherm was reduced. The width of the thermal plume increased somewhat. Fig. 11 shows the comparison of surface isotherms obtained by the model prediction and I.R. measurement data. In general, the model prediction is observed to be in relatively good agreement with I.R. measurements.

(F) SUMMARY

The present study predicts the three-dimensional flow and temperature field in the receiving body of ocean water owing to the submerged discharge near the ocean floor. The effects of currents, wind, surface cooling, and bottom topography are combined in this complete field numerical model. The

vertical and horizontal stretching provide more efficient use of this model and ease of boundary condition specification. The results from the model obtained indicate proper numerical behavior of the model. It can be concluded that the physical behavior of the plume is reproduced by the model with relatively good agreement. Further calbiration efforts are still continuing. Some field experimental data will be obtained for using the final verification of the model.

(G) ACKNOWLEDGEMENTS

Authors of this paper would like to express their sincerest appreciation to Dr. M. Estoque for his many helpful suggestions and discussions in this work.

The research was sponsored by NASA under contract NAS10-8926.

REFERENCES

1. Lee and Sengupta, "Three-Dimensional Thermal Pollution Model", Detailed Technical Report to NASA, CR. No. 144858 Dept. of Mech. Engineering, Univ. of Miam, Dec.,1976.

2. Freeman, N.G., "A Modified Sigma Equations' Approach to the Numerical Modeling of Great Lakes Hydrodynamics", Journal of Geo. Research, Vol. 72, No. 6, Feb., 1972.

3. Waldrop, W.R., "Three-Dimensional Flow and Sediment Transport at River Mouths", Technical Report No. 150, Louisiana State University, Sept., 1973.

4. "Environmental Statement Related to the St. Lucie Plant Unit No. One", Florida Power and Light Company, June, 1973.

5. Parker and Krenkel, "Physical and Egnineering Aspects of Thermal Pollution", CRC Press, L970.

6. Phillips, N.A., "A Co-ordinate System Having Some Special Advantages for Numerical Forecasting", J. Meteorology, 14,1957.

7. Dunn, Policastro, & Paddock, "Evaluation of Mathematical Models for the Near and Complete Field", Argonne Nat. Laboratory, Report ANL/WR-75-3, August, 1975.

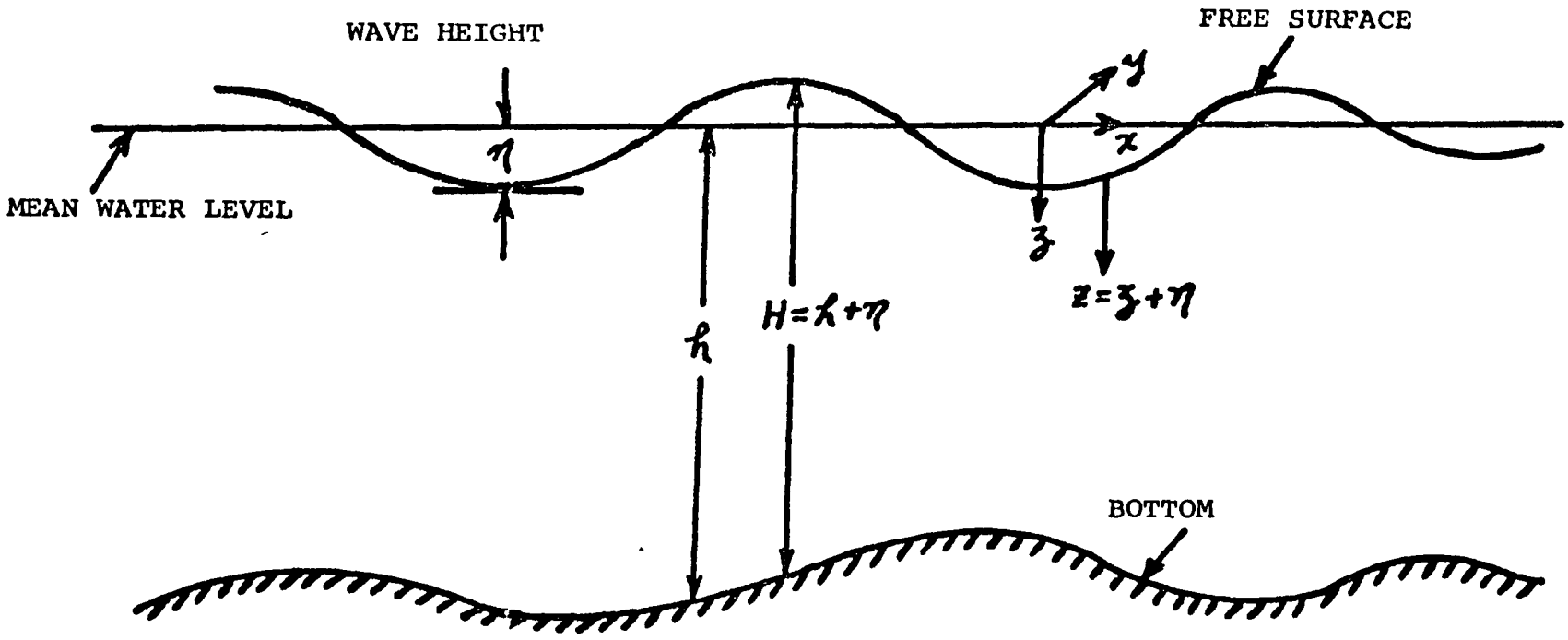

FIG: (1) The xyz Coordinate System for the Free-Surface Model

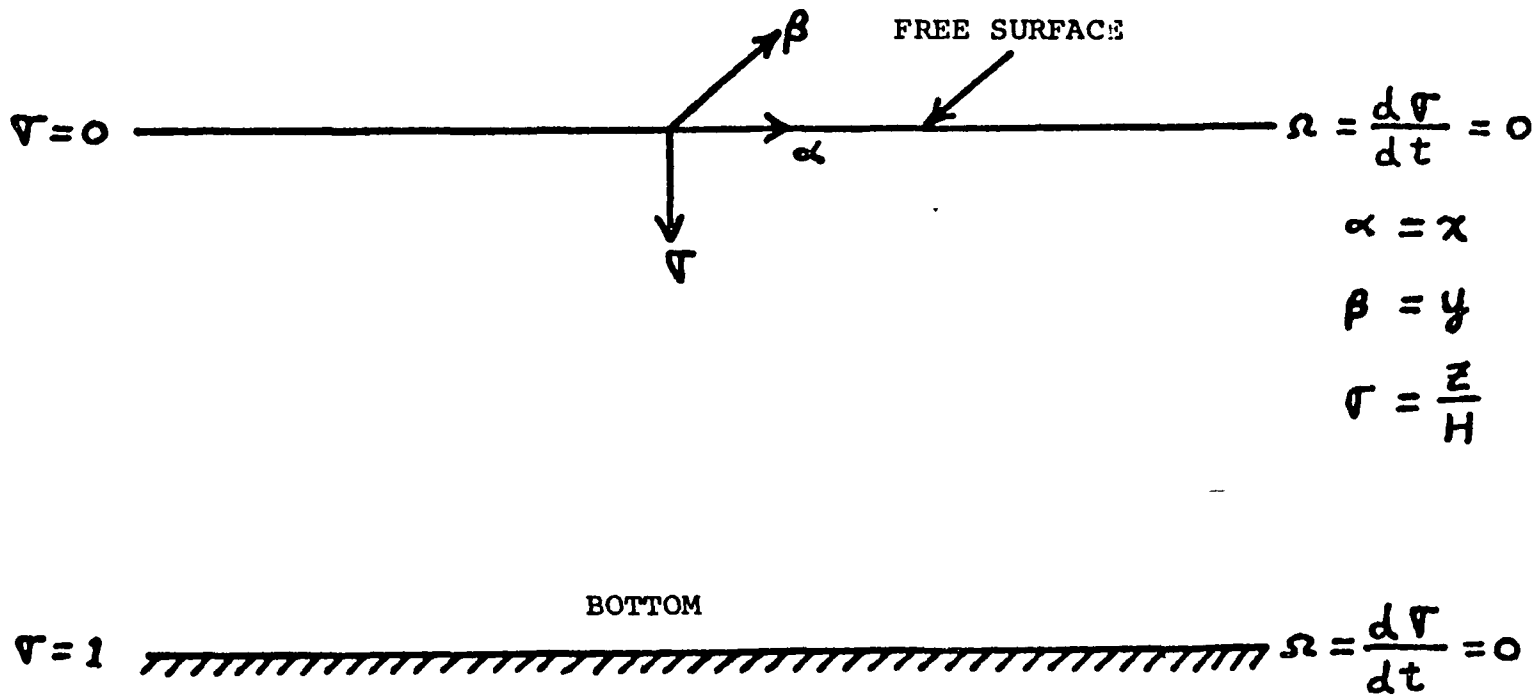

FIG: (2) The αβσ Coordinate System for the Free-Surface Model

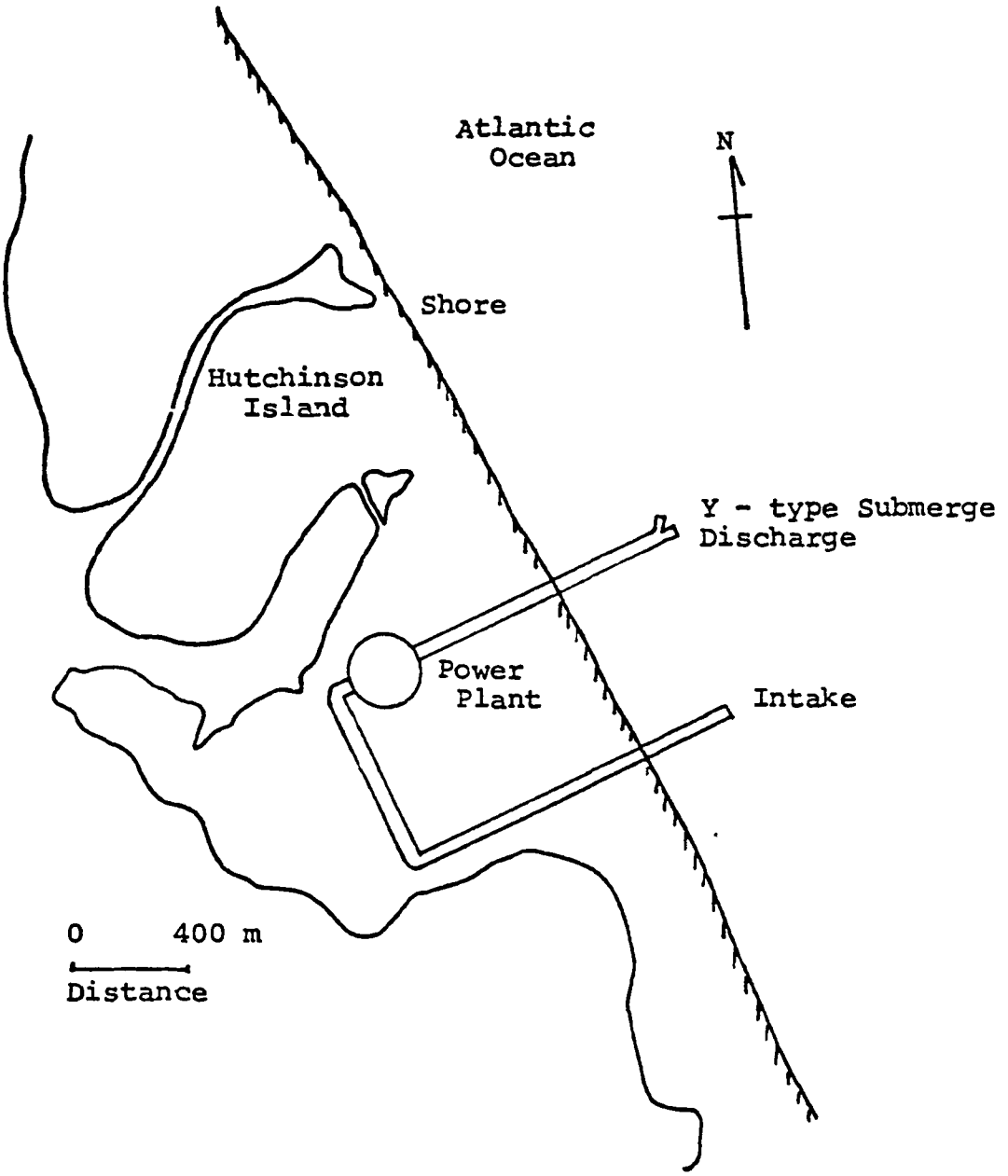

Fig. (3) Florida Power and Light Company's Hutchinson Island Site Power Plant

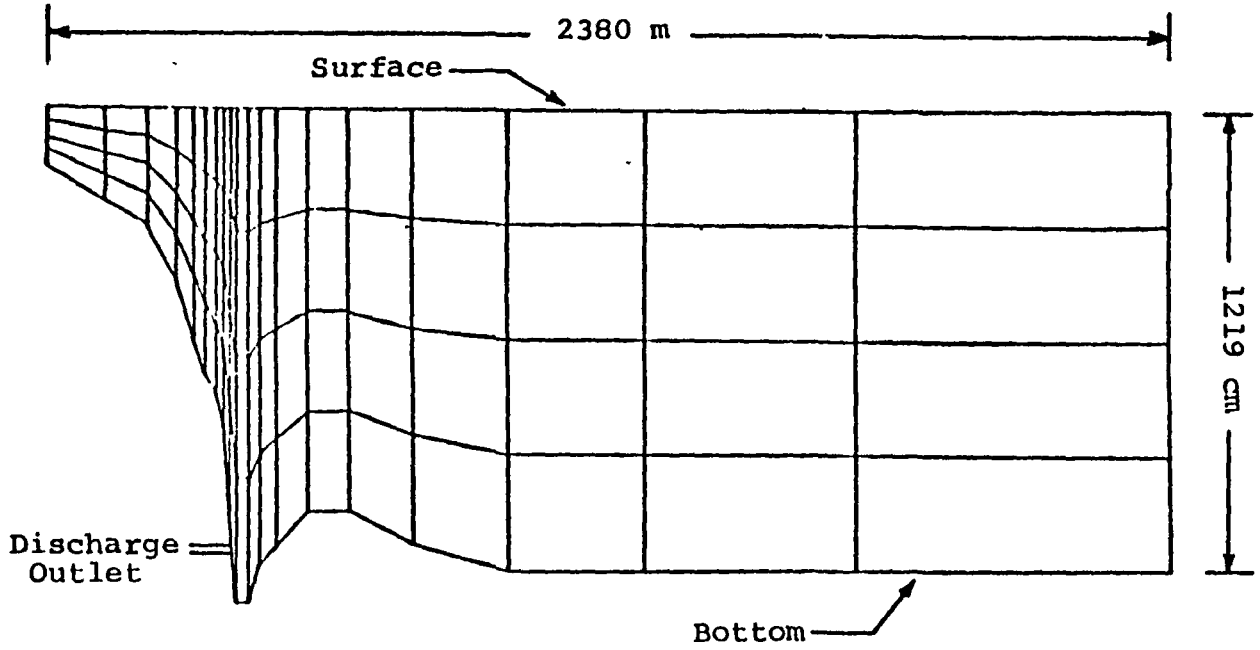

Fig.(4) : Distorted Vertical Section With Sigma Stretching For Free Surface Near Field Model Applied to Hutchinson Island Site

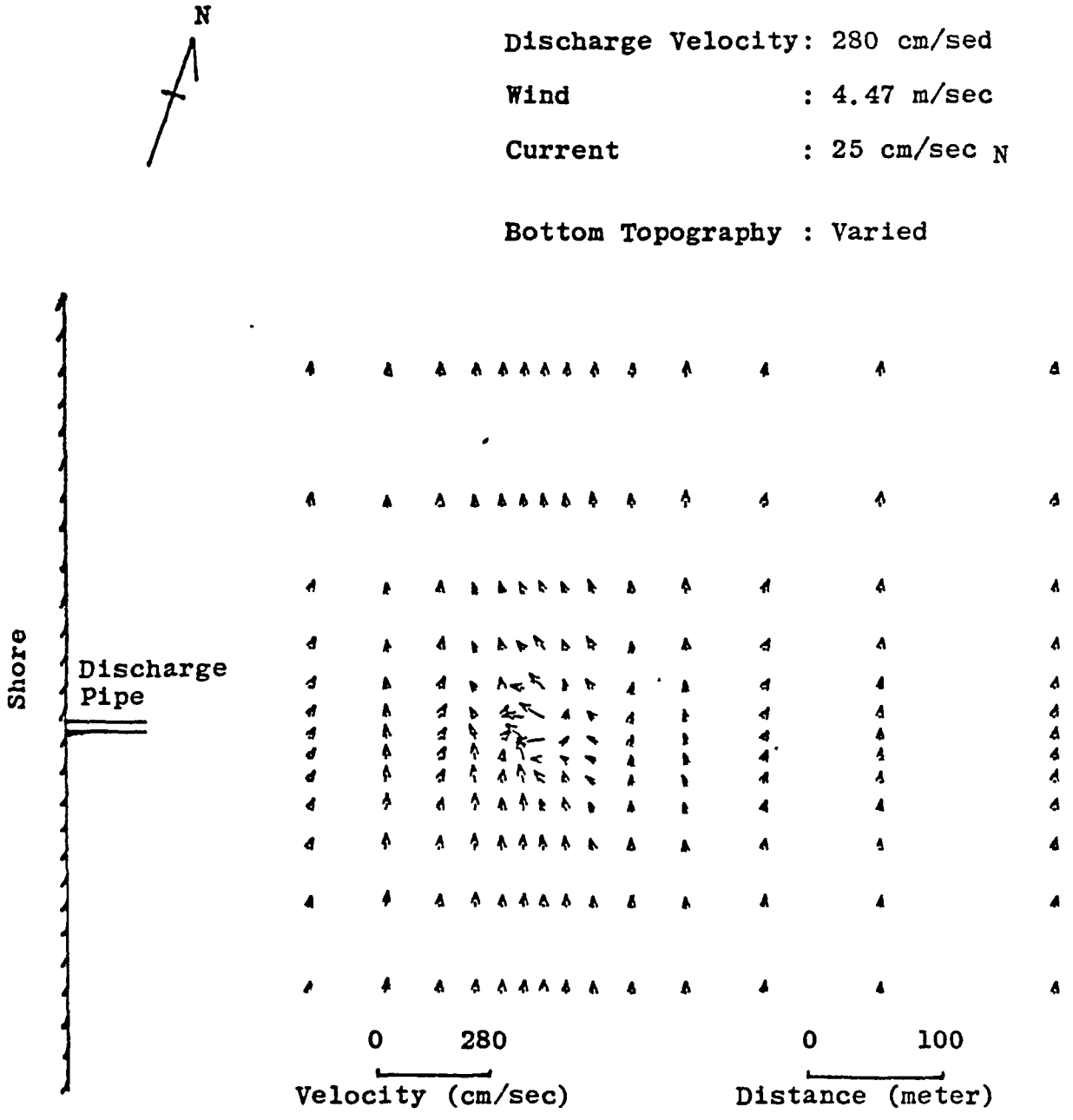

Fig. (5) Surface velocity distribution with current, wind and bottom topography at Hutchinson Island Site (Free Surface Model)

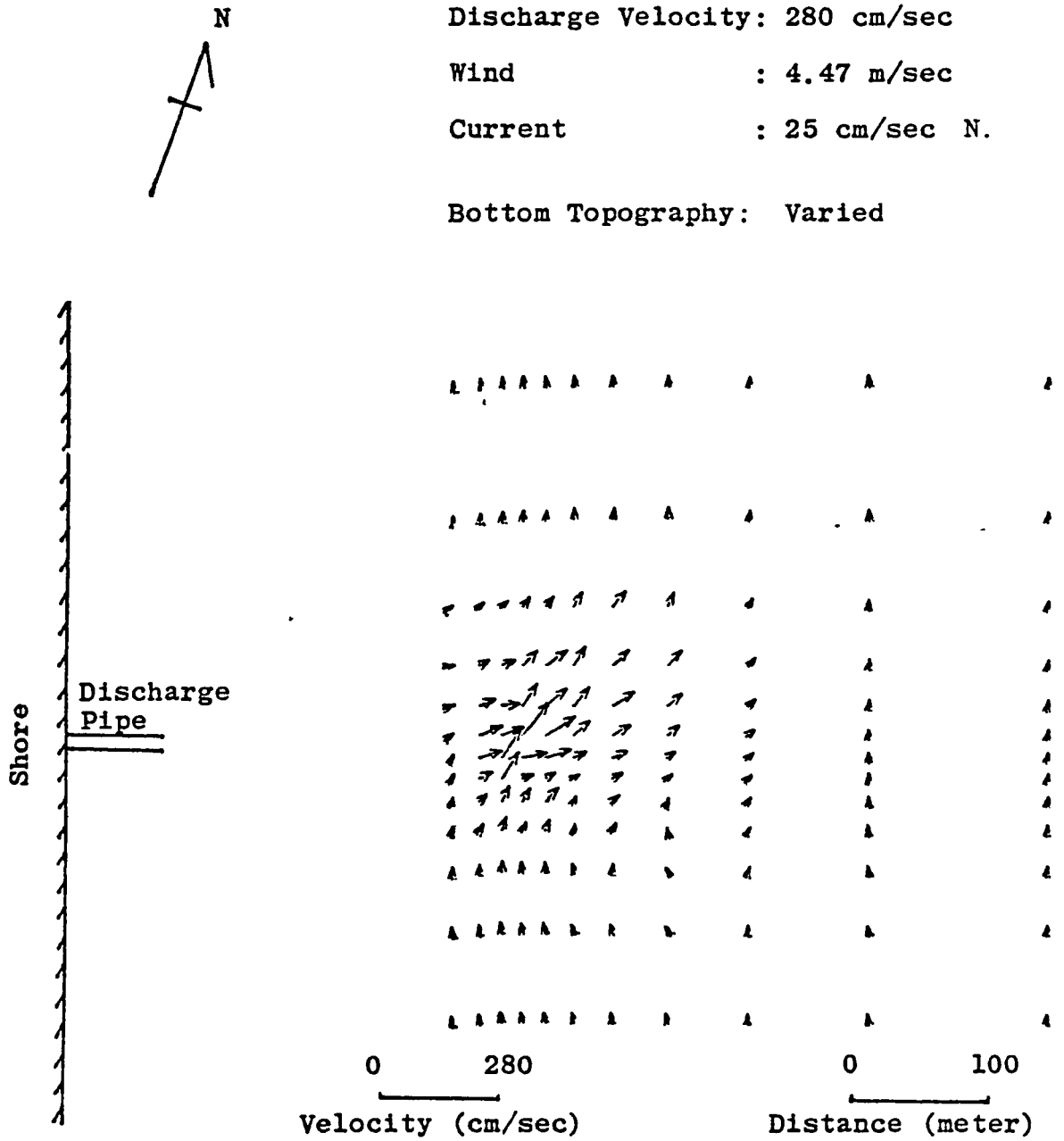

Fig. (6) Horizontal velocity distribution at the plant 6.5 meter below the free surface with current. wind and bottom topography at Hutchinson Island Site (Free Surface Model)

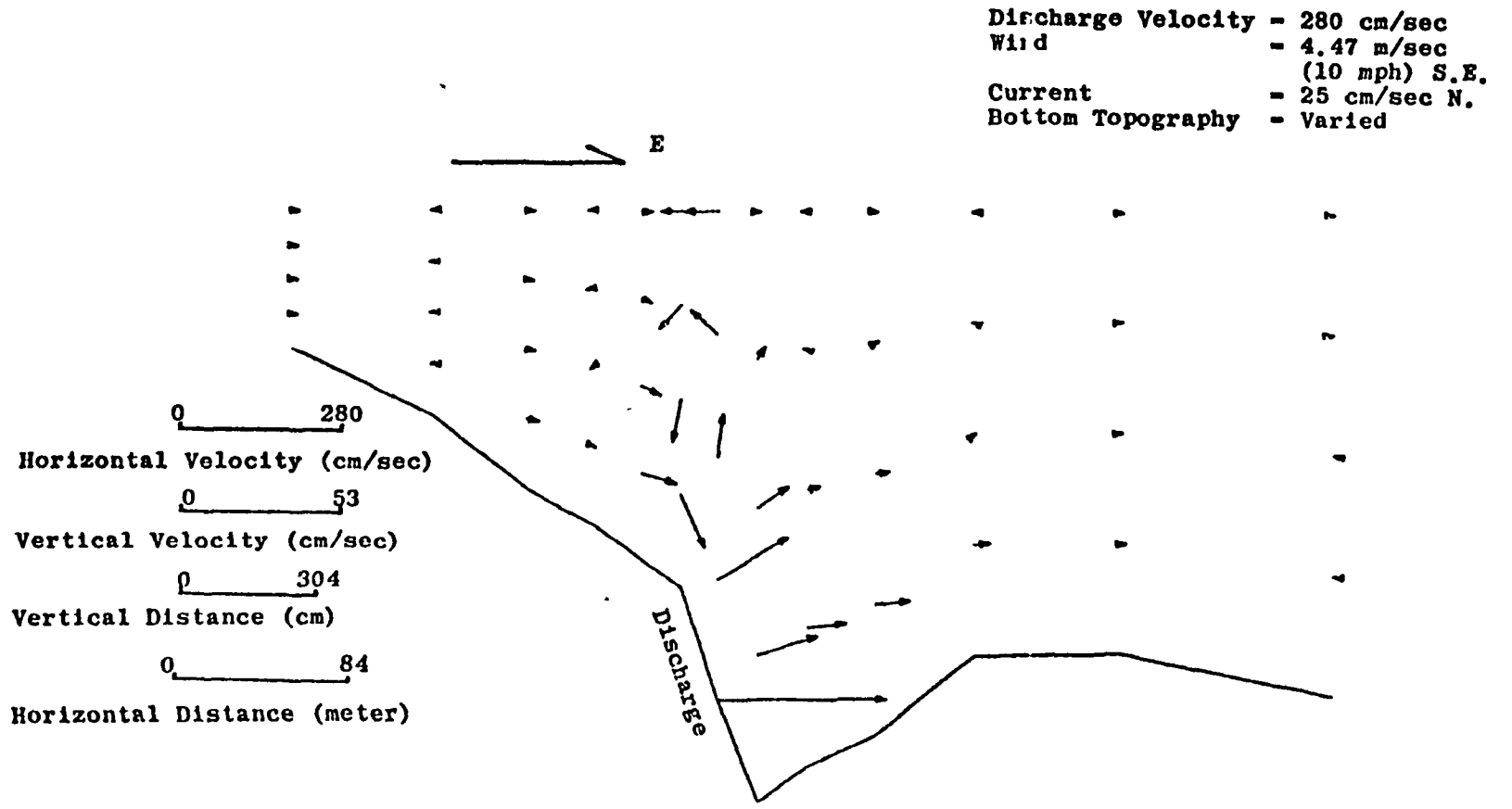

Fig. (7) Velocity distribution at section J-11 for Hutchinson Island Site with vertical scale exaggerated 5.25 times (Free Surface Model)

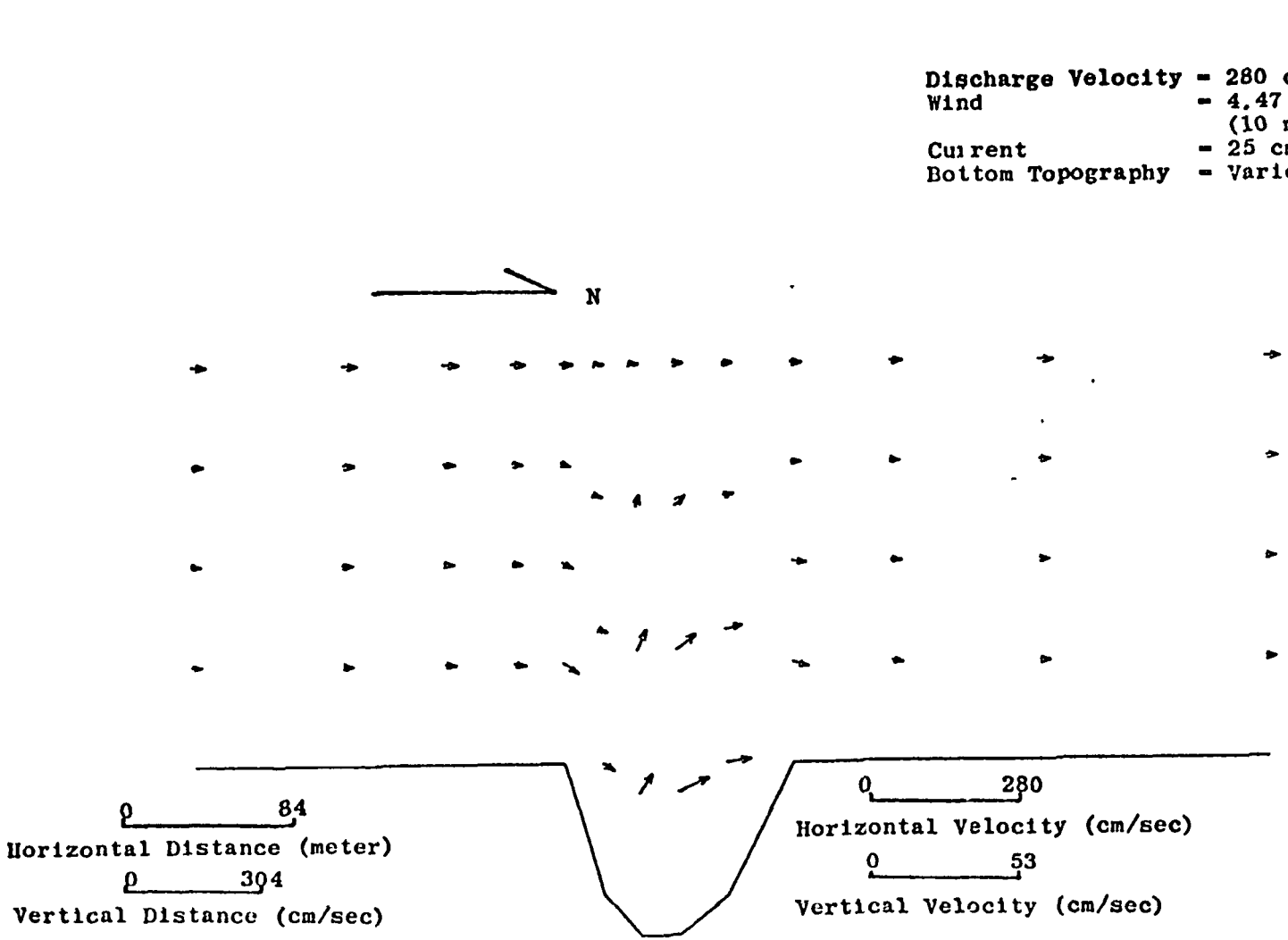

Fig.(8) -- Velocity distribution at section I-10 for Hutchinson Island Site with vertical scale exaggerated 5.25 times (Free Surface Model)

Discharge Velocity : 280 cm/sec
Wind : 4.47 m/sec
(10 mph) S.E.
Current : 25 cm/sec N.
Bottom Topography : Varied

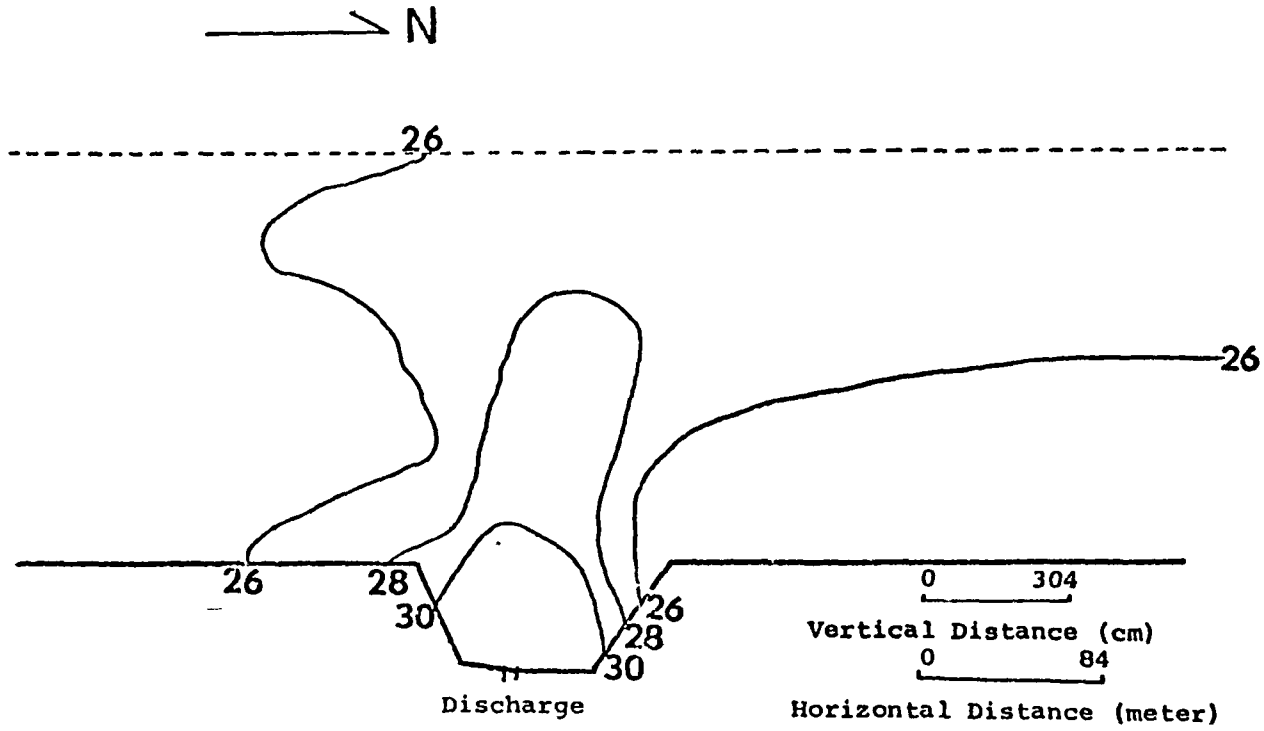

Fig. (9) Vertical isotherms at section I=9 for the Hutchinson Island Site (Free Surface Model)

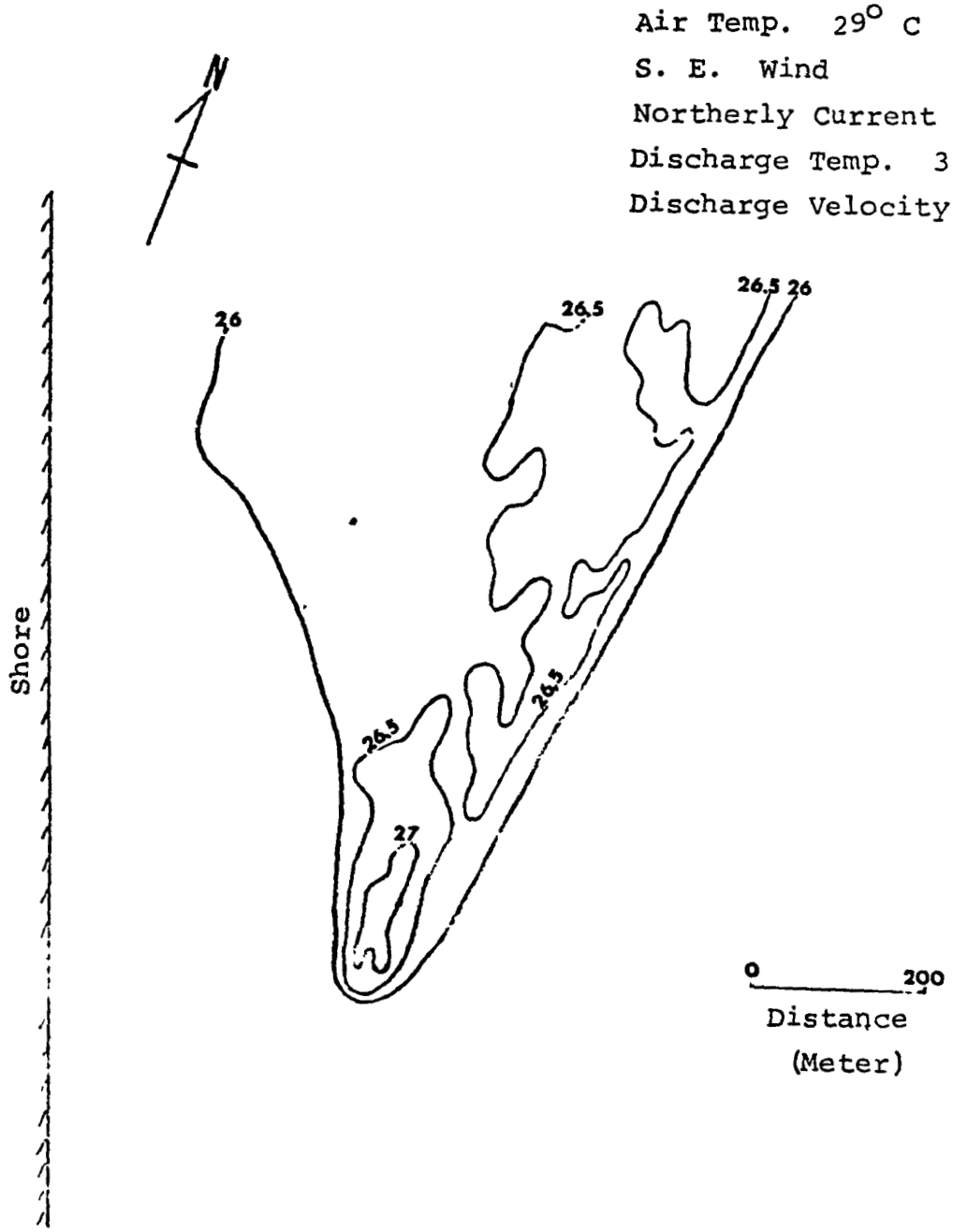

Fig. (10) Surface Isotherms from I.R. Data at Hutchinson Island Power Plant, 2 June 1976, 1048-1059 EST

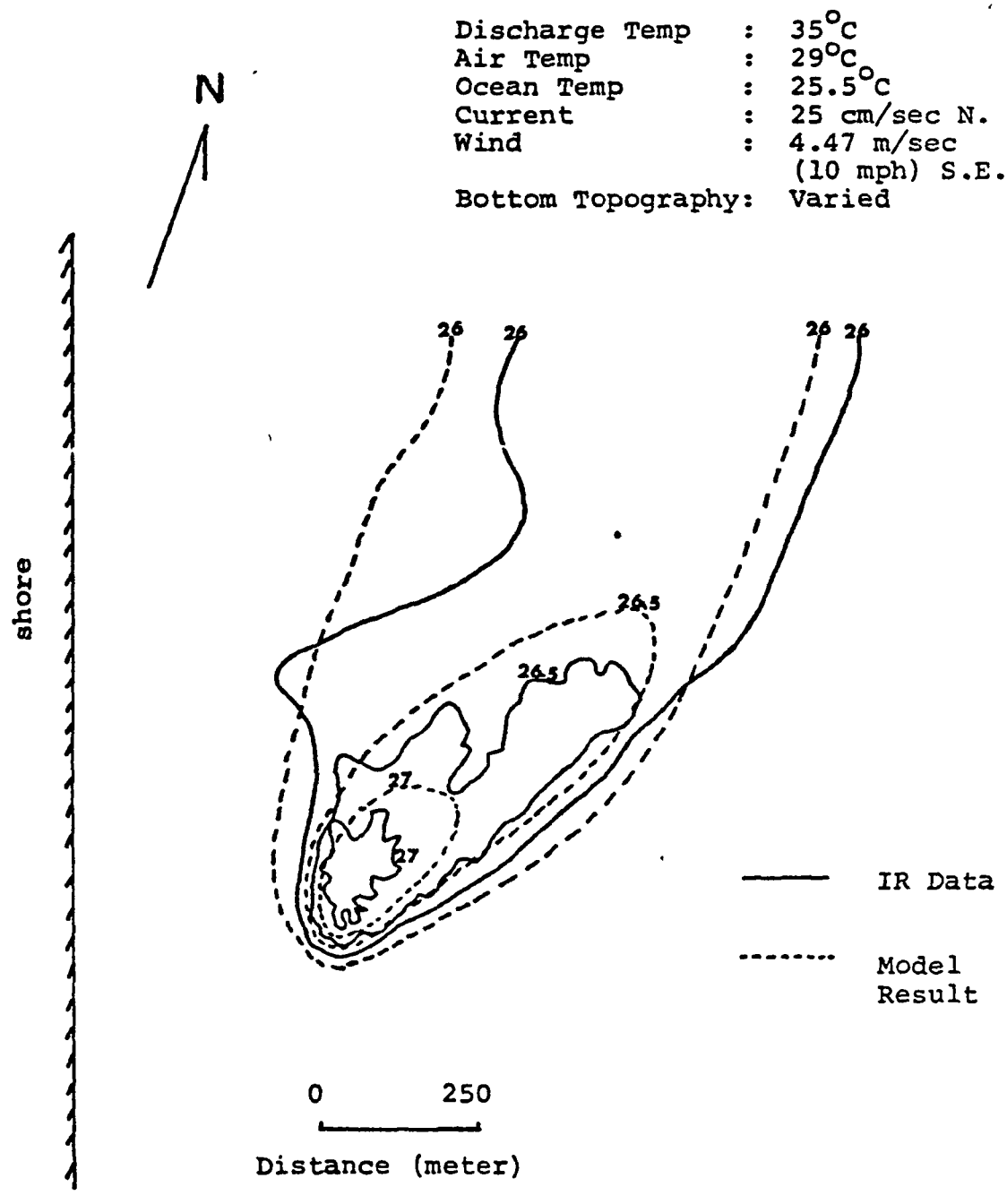

Fig.(11) Comparison of model results and afternoon IR data at Hutchinson Island Site for June 2, 1976 (Free Surface Model)